

Shortcuts Everywhere and Nowhere: Exploring Multi-Trigger Backdoor Attacks

Yige Li^{1,2} Jiabo He² Hanxun Huang³ Jun Sun⁴ Xingjun Ma¹

Abstract

Backdoor attacks have become a significant threat to the pre-training and deployment of deep neural networks (DNNs). Although numerous methods for detecting and mitigating backdoor attacks have been proposed, most rely on identifying and eliminating the “shortcut” created by the backdoor, which links a specific source class to a target class. However, these approaches can be easily circumvented by designing multiple backdoor triggers that create shortcuts everywhere and therefore nowhere specific. In this study, we explore the concept of Multi-Trigger Backdoor Attacks (MTBAs), where multiple adversaries leverage different types of triggers to poison the same dataset. By proposing and investigating three types of multi-trigger attacks including *parallel*, *sequential*, and *hybrid* attacks, we demonstrate that 1) multiple triggers can coexist, overwrite, or cross-activate one another, and 2) MTBAs easily break the prevalent shortcut assumption underlying most existing backdoor detection/removal methods, rendering them ineffective. Given the security risk posed by MTBAs, we have created a multi-trigger backdoor poisoning dataset to facilitate future research on detecting and mitigating these attacks, and we also discuss potential defense strategies against MTBAs.

1. Introduction

Deep neural networks (DNNs) have become the standard models for tasks in computer vision (He et al., 2016; Dosovitskiy et al., 2021), natural language processing (Devlin et al., 2019; Mann et al., 2020), and speech recognition (Chan et al., 2016). However, research has demonstrated that DNNs are susceptible to backdoor attacks (Gu et al., 2017; Chen et al., 2017; Li et al., 2020), where stealthy

This work was partially done when Yige Li interned at Bosch Research Asia Pacific.¹Fudan University²Bosch Research Asia Pacific & Bosch Center for Artificial Intelligence (BCAI)³The University of Melbourne⁴Singapore Management University. Correspondence to: Xingjun Ma <xingjunma@fudan.edu.cn>.

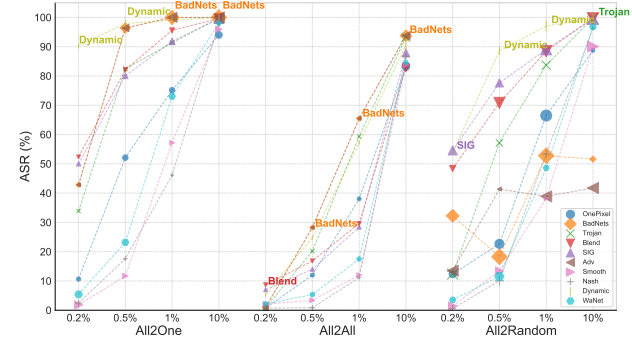


Figure 1. Effectiveness of multi-trigger attacks at various poisoning rates (0.2% ~ 10%) under 3 labeling modes (All2One, All2All, and All2Random) on the CIFAR-10 dataset. The results of All2One and All2All show that 1) different triggers can largely coexist at 10% poisoning rate with high attack success rates (ASRs) but exhibit varied ASRs at extremely low poisoning rate (0.2%).

triggers are embedded into the target models during training by poisoning a small subset of the training data or altering the training process. In image classification, this typically involves adding a fixed, carefully crafted trigger pattern to a few training images that the adversary can access. The objective of a backdoor attack is to manipulate the model into producing a specific output chosen by the adversary whenever the trigger pattern appears in a test input. With the increasing use of large models pre-trained on unsupervised web data or those provided by untrusted sources, concerns about the backdoor vulnerability of these models have grown, particularly when they are used in safety-critical applications.

Given the significant security threat posed by backdoor attacks on neural networks, a variety of backdoor detection and removal techniques have been developed. Some prominent methods include (Wang et al., 2019; Li et al., 2021c; Wu & Wang, 2021; Li et al., 2023). These methods generally operate under the assumption that backdoor triggers are unknown in practice. As a result, they focus on identifying backdoors by detecting the presence of “shortcuts” between a specific source class and a target class, and then mitigating the threat by eliminating these shortcuts. However, in this work, we systematically demonstrate that such approaches can be effectively bypassed by implementing multiple back-

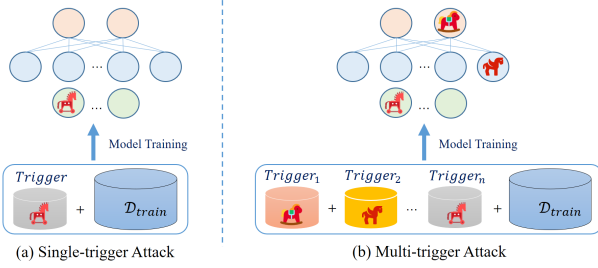


Figure 2. An illustrative comparison between single-trigger and multi-trigger backdoor attacks.

door triggers that create shortcuts in all directions, rendering them indistinguishable and making it challenging to target any specific one for removal. This strategy exposes a critical vulnerability in existing backdoor defenses, highlighting the need for more robust and comprehensive protection mechanisms.

In this work, we extend traditional single-trigger backdoor attacks to multi-trigger backdoor attacks. Note that we do not call them *multi-adversary attacks* as our focus is on the triggers, demonstrating that even a single adversary can simultaneously employ multiple distinct triggers to poison a dataset. We explore three distinct implementation strategies for multi-trigger backdoor attacks: *parallel*, *sequential*, and *hybrid*, where the latter blends multiple trigger patterns into a single, more potent super trigger pattern. Furthermore, we conduct a thorough analysis of 10 different existing triggers, uncovering their *coexistence*, *overwriting*, and *cross-activation* effects. Our findings reveal that: 1) different backdoor triggers can coexist within the same dataset, whether injected in parallel or sequentially; 2) certain triggers can overwrite others even at minimal poisoning rates (as low as 0.2% or 0.5%); 3) one trigger can cross-activate another in sequential attack settings; and 4) different trigger patterns can be combined into a hybrid trigger to enhance attack efficacy. Figure 1 summarizes some of the experimental results. These insights highlight the heightened security risks posed by the presence of multiple backdoor adversaries.

Next, we systematically evaluate existing backdoor defense methods since they have not been adequately evaluated against multi-trigger attacks. This gap in evaluation can lead to overly optimistic perceptions of backdoor robustness and a false sense of security. Our findings confirm this vulnerability: multi-trigger backdoor attacks can severely undermine the effectiveness of current state-of-the-art backdoor detection and removal techniques. Specifically, 1) widely used detection methods like Neural Cleanse (NC) (Wang et al., 2019) struggle to identify multi-trigger attacks, and 2) mainstream backdoor removal techniques such as fine-tuning (Liu et al., 2018a), Neural Attention Distillation (NAD) (Li et al., 2021c), Adversarial Neuron Pruning

(ANP) (Wu & Wang, 2021), Reconstructive Neuron Pruning (RNP) (Li et al., 2023), and Anti-Backdoor Learning (ABL) fail to effectively purify models compromised by multiple triggers. The challenge of identifying multiple triggers (or the correct sequence to defend against them) is compounded by the difficulty of determining the exact number of triggers present, making defense against multi-trigger attacks extremely difficult.

Our main contributions are as follows.

- We introduce the concept of multi-trigger backdoor attacks to expose the limitations of existing “shortcut”-based backdoor detection and removal methods. We highlight the practical threat posed by such attacks in real-world scenarios, where a dataset or model could be simultaneously attacked by multiple adversaries using parallel, sequential, or hybrid triggers.
- Through more than 200 experiments involving 10 types of triggers, 3 poisoning strategies (parallel, sequential, and hybrid-trigger), 4 poisoning rates (ranging from 0.2% to 10%), 3 label modification strategies (All2One, All2All, and All2Random), 2 datasets (CIFAR-10 and an ImageNet subset), and 4 DNN architectures (including 2 CNNs and 2 ViTs), we uncover the coexistence, overwriting, and cross-activation effects of multi-trigger backdoor attacks.
- By re-evaluating 8 existing backdoor defense methods (4 for detection and 4 for removal) against multi-trigger backdoor attacks with 10 types of triggers, we demonstrate that: 1) all detection methods struggle with All2All and All2Random attacks, though they show some effectiveness against All2One attacks; 2) none of the detection methods can accurately identify the target of multi-trigger attacks; and 3) no backdoor removal method is capable of fully eliminating any of the 10 triggers.
- We have built and released a multi-trigger backdoor dataset to support future research on backdoor attacks and defenses.

2. Related Work

Backdoor Attack A backdoor attack designs a trigger pattern to achieve a high attack success rate while being stealthy to humans. Existing backdoor triggers can be categorized into dataset-wise vs. sample-wise triggers. A dataset-wise trigger applies the same trigger pattern to all poisoned samples while a sample-wise trigger poisons each sample with a unique trigger pattern. Examples of dataset-wise triggers include one pixel (Tran et al., 2018), a checkerboard pattern (Gu et al., 2017), a global pattern like Gaussian noise (Chen et al., 2017), background reflection (Liu et al., 2020), to

name a few. Compared to dataset-wise triggers, sample-wise triggers can be more complex (and stealthy) as they are often optimized by additional techniques. For instance, generative model-based backdoor attacks (Lin et al., 2020; Nguyen & Tran, 2020; Cheng et al., 2021; Li et al., 2021a) generate backdoor trigger patterns adaptively based on different input samples. Regardless of the diverse trigger patterns, all existing backdoor attacks follow a *single-trigger attack setting*, where there exists only one adversary and one single type of trigger (Li et al., 2022). Such a restricted setting limits the exploration of backdoor attacks in more realistic settings where multiple adversaries could attack the same dataset. It also raises the question as to whether these attacks can coexist and be simultaneously effective when leveraged by different adversaries to poison the same dataset. In this paper, we explore such an aspect of a diverse set of existing triggers under a more realistic setting: *multi-trigger attack setting* where there are multiple adversaries and types of triggers.

Backdoor Defense Existing backdoor defenses can be categorized into backdoor detection and backdoor removal (or mitigation) methods. Detection methods identify whether a given model has been backdoored by a backdoor attack (Chen et al., 2019; Wang et al., 2019; Guo et al., 2019; Xu et al., 2021) or whether a sample contains a backdoor trigger (Tran et al., 2018; Chen et al., 2019; Gao et al., 2019; Zeng et al., 2021; Huang et al., 2023).

Removal methods aim to eliminate the backdoor trigger (if it exists) from the model without affecting its functionality. This can be done during the training process via anti-backdoor learning (Li et al., 2021b; Huang et al., 2022), or later on via fine-tuning, fine-pruning (Liu et al., 2018a), distillation (Li et al., 2021c), adversarial pruning (Wu & Wang, 2021), channel Lipschitzness based pruning (Zheng et al., 2022), or reconstructive pruning (Li et al., 2023). However, all of these defenses were developed for single-trigger attacks, thus facing high uncertainty when applied to defend multi-trigger attacks. In this paper, we run extensive experiments to reexamine the effectiveness of these defenses to multi-trigger backdoor attacks.

3. Multi-Trigger Backdoor Attacks

We first introduce our threat model and definition of backdoor attacks and then introduce the three types of multi-trigger backdoor attacks proposed in this work.

3.1. Threat Model and Problem Definition

Threat Model Our threat model introduces 3 poisoning strategies for multi-trigger attacks: **parallel**, **sequential**, and **hybrid**, covering scenarios involving both independent and collusive adversaries. Specifically, there exist one or more

adversaries where each adversary can access a few training samples but none of them can manipulate the training procedure. The adversaries can be independent or collusive, with independent adversaries poisoning different training samples with different types of triggers, while collusive adversaries could poison the same training samples in sequential order by stacking one trigger after another. There could also exist a super adversary that launches the above attacks altogether or combines multiple triggers into a hybrid trigger.

Definition of Backdoor Attack We focus on image classification tasks. Given a clean training dataset $\mathcal{D} = \{(\mathbf{x}_i, y_i)\}_{i=1}^N$, where $\mathbf{x}_i \in \mathcal{X}$ represents a training image and $y_i \in \mathcal{Y}$ is its label. A backdoor adversary generates backdoor examples with a triggering function $tr : \mathcal{X} \rightarrow \mathcal{X}$. For each clean sample, it maps the sample \mathbf{x} into a backdoor sample \mathbf{x}_b , i.e., $\mathbf{x}_b = tr(\mathbf{x})$ and modifies its label to a backdoor target label y_b . To ensure stealthiness and efficacy for backdoor injection, the adversary randomly chooses a few training samples to poison, which creates a set of backdoor samples $\mathcal{D}_b = \{(\mathbf{x}_b, y_b)\}$. As we mentioned earlier, most existing attacks only inject a single type of backdoor trigger into the training data, meaning there is only one triggering function $tr(\cdot)$. We call these attacks *Single-Trigger Backdoor Attacks (STBAs)*. The final poisoned training dataset can be denoted as $\hat{\mathcal{D}} = \mathcal{D}_c \cup \mathcal{D}_b$, where $\mathcal{D}_c = \{(\mathbf{x}_c, y_c)\}$ represents clean samples and clean labels, while $\mathcal{D}_b = \{(\mathbf{x}_b, y_b)\}$ represents backdoor samples and backdoor labels. The poisoning rate is defined as $\alpha = |\mathcal{D}_b|/|\hat{\mathcal{D}}|$. Training a model on $\hat{\mathcal{D}}$ is solving the following optimization problem:

$$\min_{\theta} \mathbb{E}_{\mathcal{D}_c} [\mathcal{L}(f_{\theta}(\mathbf{x}_c), y_c)] + \mathbb{E}_{\mathcal{D}_b} [\mathcal{L}(f_{\theta}(\mathbf{x}_b), y_b)], \quad (1)$$

where \mathcal{L} is the cross-entropy loss. The first term in the above objective formulates the loss of the clean (original) task, while the second term formulates the loss of the backdoor task. Training on the dataset can be viewed as a process where the model learns both tasks.

Definition of Multi-Trigger Backdoor Attack We call backdoor attacks that utilize multiple types of triggers (possibly from one or more adversaries) to attack the same dataset termed *Multi-Trigger Backdoor Attacks (MTBAs)*. Figure ?? illustrates the idea of MTBA. Note that we did not call these attacks multi-adversary attacks as even one adversary could implement different types of triggers. The MTBA problem can also be formulated as Eq. (1), but with a slightly more complex poisoning set that contains multiple triggers:

$$\mathcal{D}_b = \bigcup_{k=1}^m \mathcal{D}_b^k = \bigcup_{k=1}^m \{(\mathbf{x}_b^k, y_b^k)\}, \quad (2)$$

where $\mathbf{x}_b^k = \text{tr}_k(\mathbf{x})$ is a poisoned sample by the k -th trigger $\text{tr}_k(\cdot)$, and \mathcal{D}_b^k is the subset of poisoned samples by trigger $\text{tr}_k(\cdot)$ for overall m triggers. For multi-trigger attacks, the poisoned dataset becomes $\hat{\mathcal{D}} = \mathcal{D}_c \cup \mathcal{D}_b$ with a poisoning rate of $\alpha = |\mathcal{D}_b|/|\hat{\mathcal{D}}| = \sum_{k=1}^m |\mathcal{D}_b^k|/|\hat{\mathcal{D}}|$.

3.2. Poisoning Strategies

Conceptually, MTBA is an extension of STBA. While STBA injects only one type of trigger into the target model, MTBA introduces multiple types of triggers. We introduce three poisoning strategies to simulate diverse real-world threat scenarios: *parallel*, *sequential*, and *hybrid-trigger*.

3.2.1. PARALLEL POISONING

Arguably, the triggers can be injected into the victim dataset by multiple independent adversaries. In this case, it is reasonable to assume that the poisoned subsets are not overlapping with each other, as two independent adversaries are of extremely low probability to poison the same sample, given the low poisoning rate. We call this poisoning strategy *parallel poisoning*.

To implement parallel poisoning, we randomly sample a few training samples into a backdoor candidate subset \mathcal{D}_s and then uniformly divide \mathcal{D}_s into m smaller subsets, i.e., $\mathcal{D}_s = \{\mathcal{D}_s^k\}_{k=1}^m$. We then assign, to each \mathcal{D}_s^k , a randomly selected trigger $\text{tr}_k \in \mathcal{T} = \{\text{tr}_k\}_{k=1}^m$ from a trigger pool, i.e., $\mathcal{D}_b^k = \{(\mathbf{x}_b^k, y_b^k) | \mathbf{x}_b^k = \text{tr}_k(\mathbf{x}_s^k), \mathbf{x}_s^k \in \mathcal{D}_s^k\}$. Accordingly, training a model on multi-trigger poisoned dataset $\{\mathcal{D}_b^k\}_{k=1}^m$ can be formulated as:

$$\min_{\theta} \mathbb{E}_{\sim \mathcal{D}_c} [\mathcal{L}(f_{\theta}(\mathbf{x}_c), y_c)] + \sum_{k=1}^m \mathbb{E}_{\mathcal{D}_b^k} [\mathcal{L}(f_{\theta}(\mathbf{x}_b^k), y_b^k)], \quad (3)$$

where \mathcal{L} is the cross-entropy loss and m is the number of independently poisoned subsets. Training on a multi-trigger backdoored dataset can be viewed as the learning process of one clean task and m backdoor tasks simultaneously.

3.2.2. SEQUENTIAL POISONING

It is also possible that different adversaries launch their attacks at different times. In this case, different adversaries may attack the same dataset in sequential order, but still on non-overlapping data subsets. We call this attacking strategy as *sequential poisoning*. This poisoning strategy allows us to study the overwriting effect of different triggers, i.e., the question of whether an early-injected trigger can stay effective in the presence of subsequent attacks.

To implement sequential poisoning, we inject different types of triggers into the victim dataset following a specific order. Suppose adversary k can poison a small subset of clean samples \mathcal{D}_s^k with its own trigger tr_k to obtain a backdoor subset \mathcal{D}_b^k , and accordingly a poisoned training dataset

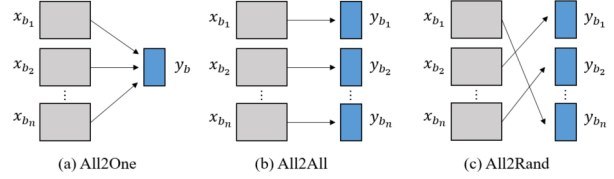


Figure 3. An illustration of the three label modification strategies.

$\hat{\mathcal{D}}_k = \mathcal{D}_c \cup \mathcal{D}_b^k = \{\mathcal{D} \setminus \mathcal{D}_s^k\} \cup \mathcal{D}_b^k$, where \mathcal{D} is the original dataset, \mathcal{D}_c is the subset of remaining clean samples, \mathcal{D}_s^k is the victim clean subset, \mathcal{D}_b^k are backdoor samples generated from \mathcal{D}_s^k . The model is then trained on the poisoned dataset to obtain a backdoored model f_{θ_k} , as follows:

$$\min_{\theta_k} \mathbb{E}_{(\mathbf{x}, y) \sim \hat{\mathcal{D}}_k} [\mathcal{L}(f_{\theta_k}(\mathbf{x}), y)]. \quad (4)$$

The next adversary $k+1$ poisoned the dataset $\hat{\mathcal{D}}_k$ following the same procedure as adversary k to obtain poisoned dataset $\hat{\mathcal{D}}_{k+1} = \mathcal{D}_c \cup \mathcal{D}_b^k \cup \mathcal{D}_b^{k+1} = \{\hat{\mathcal{D}}_k \setminus \mathcal{D}_s^{k+1}\} \cup \mathcal{D}_b^{k+1}$. The backdoored model f_{θ_k} is then continuously trained on $\hat{\mathcal{D}}_{k+1}$ to produce $f_{\theta_{k+1}}$, as follows:

$$\min_{\theta_{k+1}} \mathbb{E}_{(\mathbf{x}, y) \sim \hat{\mathcal{D}}_{k+1}} [\mathcal{L}(f_{\theta_{k+1}}(\mathbf{x}), y)]. \quad (5)$$

After the above sequential training, model $f_{\theta_{k+1}}$ becomes a sequentially backdoored model that contains both trigger tr_k and trigger tr_{k+1} .

Note that, although the adversaries follow a sequential order, we assume they are independent and their selected victim subsets do not overlap ($\mathcal{D}_s^k \cap \mathcal{D}_s^{k+1} = \emptyset$) and only contain clean samples. These are reasonable assumptions because: **1**) the adversaries have access to the victim samples, thus can easily ensure that they are clean (so would not impact trigger injection); and **2**) independent attackers often own different samples. We also assume the subsequent adversary trains the backdoored model on the basis of the previous backdoored model. This is to simulate the current trend of fine-tuning large models, where a victim user may download and fine-tune a pre-trained (and poisoned by a previous adversary) large model for its own downstream application.

3.2.3. HYBRID-TRIGGER POISONING

There may also exist a super adversary that combines different triggers into one hybrid trigger to achieve the effect of multiple triggers. This poisoning strategy is realistic because the current literature already has a large number of trigger patterns for the adversary to exploit. We call this poisoning strategy as *hybrid-trigger poisoning*.

In contrast to parallel and sequential poisonings, which are based on multiple independent triggers, hybrid-trigger poisoning represents a sample-wise attacking strategy. It simultaneously introduces multiple distinct triggers into one

single input sample, endowing it with multi-trigger characteristics. Specifically, given a clean sample \mathbf{x} , a hybrid-trigger attack poisons the sample with m elementary triggers $\mathcal{T} = \{\text{tr}_k\}_{k=1}^m$ as follows:

$$\mathbf{x}_h = \text{tr}_m \circ \text{tr}_{m-1} \circ \cdots \circ \text{tr}_1(\mathbf{x}), \quad (6)$$

where, we use soft blending at each step, i.e., $\text{tr}_k \circ \text{tr}_{k-1}(\mathbf{x}) = \lambda \cdot \text{tr}_k + (1 - \lambda) \mathbf{x}_b^{k-1}$ (we set $\lambda = 0.25$ in our experiments). Suppose the training dataset is \mathcal{D} and the small subset of clean samples accessible to the adversary is $\mathcal{D}_s \subset \mathcal{D}$, the adversary injects the hybrid trigger into \mathcal{D}_s to obtain the backdoor subset $\mathcal{D}_h = \{(\mathbf{x}_h, y_h)\}$ following Eq. (6). The poisoned dataset can then be defined as $\hat{\mathcal{D}} = \mathcal{D}_c \cup \mathcal{D}_h = \{\mathcal{D} \setminus \mathcal{D}_s\} \cup \mathcal{D}_h$. The adversary can then train a backdoored model on $\hat{\mathcal{D}}$ following:

$$\min_{\theta} \mathbb{E}_{\mathcal{D}_c} [\mathcal{L}(f_{\theta}(\mathbf{x}_c), y_c)] + \mathbb{E}_{\mathcal{D}_h} [\mathcal{L}(f_{\theta}(\mathbf{x}_h), y_h)]. \quad (7)$$

Candidate Triggers Gathering a representative and meaningful set of triggers \mathcal{T} is crucial for our study. By investigating the current literature, we meticulously selected 10 types of triggers used in mainstream backdoor attacks as our candidate triggers, which include both dataset-wise triggers (such as one pixel, a checkerboard pattern, and adversarial perturbation) and sample-wise triggers (such as input-aware pattern and image deformation). A detailed list of the studied triggers can be found in Section 4.1.

3.3. Label Modification

In the context of multi-trigger backdoor attacks, different adversaries may share the same backdoor target if it is of general interest, or they may have entirely different (or random) target labels. Following prior works (Gu et al., 2017; Xue et al., 2020), we explore the following three label modification strategies, including *All2One*, *All2All*, and *All2Random* (see Figure 3).

- **All2One:** This strategy relabels all backdoor samples to a fixed backdoor target label y_t , i.e., all samples $\mathbf{x}_{b/h} \in \mathcal{D}_{b/h}$ have the same label y_t . In other words, all adversaries share the same backdoor target.
- **All2All:** It modifies the label of a backdoor sample \mathbf{x}_b (crafted from clean sample \mathbf{x}) to $y_b = (y + 1)\%K$, where K is the total number of classes, y is the original (clean) label of \mathbf{x}/\mathbf{x}_b and y_b is its modified label. This is to simulate the scenario where the next class is of particular interest to all adversaries.
- **All2Random:** This strategy simulates the scenarios where there exists no common target between the adversaries and each label has an equal chance to be selected as the target label. In this case, we modify the label of a backdoor sample \mathbf{x}_b to $y_b = \text{Random}(\{1, 2, \dots, K\})$ where $\text{Random}(\cdot)$ is a random function.

4. Experiments

In this section, we experiment and summarize the set of key findings obtained with multi-trigger attacks, including the *coexisting*, *overwriting*, and *cross-activating* effects of different triggers under parallel, sequential, and hybrid-trigger settings, and the reliability of existing defenses in the presence of multi-trigger attacks.

4.1. Experimental Setting

We choose 10 representative triggers from the current literature as our candidate triggers, which include *static triggers* like OnePixel (Tran et al., 2018), BadNets (Gu et al., 2017), Trojan attack (Liu et al., 2018b), *global triggers* like Blend (Chen et al., 2017), Sinusoidal Spectrum (SIG) (Barni et al., 2019), adversarial noise (Adv) (Turner et al., 2019), Smooth (Zeng et al., 2021), Nashivell filter (Nash) (Liu et al., 2019), and *sample-wise triggers* like Dynamic (Nguyen & Tran, 2020), WaNet (Nguyen & Tran, 2021). To ensure a consistent and fair comparison, we employ a dirty-label poisoning setup for all triggers, which includes data poisoning and label modification in two steps. We test all triggers for the parallel, sequential, and hybrid-trigger poisoning strategies and All2One, All2All, and All2Random label modification strategies. For the target model, we mainly focus on two classical CNN architectures, including ResNet (He et al., 2016) and MobileNet (Howard et al., 2017), and two Transformer architectures including ViT-base (Dosovitskiy et al., 2021) and ViT-small. The four architectures are the most widely adopted models in standard, resource-limited, or large-scale computer vision applications. Moreover, there is little study of backdoor attacks and defenses with ViTs. We fill this gap through comprehensive studies with two ViT architectures. For the datasets, we consider two commonly adopted image datasets in the field: CIFAR-10 and an ImageNet (Deng et al., 2009) subset (the first 20 classes). Unless otherwise stated, we set the poisoning rate to 10% (1% for each type of trigger). Detailed attack settings can be found in the appendix. The generated multi-trigger datasets will be released to help the development of more advanced backdoor defenses. Also, the poisoned datasets can continue to incorporate more advanced and future triggers following our findings.

For backdoor defense, we consider 8 advanced defense methods, including 4 backdoor model detection methods: Neural Cleanse (NC) (Wang et al., 2019), UMD (Xiang et al., 2023), MMDB (Wang et al., 2023), and the unlearning-based detection in RNP (RNP-U) (Li et al., 2023), and 4 backdoor removal methods: Fine-tuning (FT), Finepruning (FP) (Liu et al., 2018a), Neural Attention Distillation (NAD) (Li et al., 2021c), and Adversarial Neural Pruning (ANP) (Wu & Wang, 2021). Since these defense methods were all originally designed for CNN architectures, we only test

Table 1. The ASR (%) of *parallel* MTBAs on CIFAR-10, averaged over the 4 model architectures. ‘10% (1%)’ represents the total (trigger-wise) poisoning rate. The best attack performances are **boldfaced**.

Label Modification	Poisoning Rate	Parallel MTBAs (averaged over 4 model architectures)											
		Clean Acc.	OnePixel	BadNets	Trojan	Blend	SIG	Adv	Smooth	Nash	Dynamic	WaNet	Average
All2One	10% (1%)	95.69	94.04	100.00	99.73	99.61	99.56	99.75	95.93	98.08	100.00	98.01	98.50
	1% (0.1%)	95.70	75.16	100.00	91.33	95.59	91.85	99.25	57.18	46.12	99.05	73.05	82.93
	0.5% (0.05%)	95.53	52.12	96.38	82.44	82.09	80.04	92.76	11.72	17.60	97.94	23.19	63.99
	0.2% (0.02%)	95.94	10.64	42.83	33.89	52.38	49.98	38.40	1.81	2.43	90.28	5.43	33.25
	Average	95.71	57.99	84.80	76.85	82.42	80.36	82.54	41.66	41.06	96.82	49.92	69.67
All2All	10% (1%)	95.11	83.25	93.75	93.20	82.80	87.85	92.75	83.80	86.75	90.65	84.65	88.04
	1% (0.1%)	95.62	38.05	65.50	59.35	29.65	28.40	64.39	12.00	11.15	57.25	17.50	38.43
	0.5% (0.05%)	95.73	12.00	28.25	20.20	16.85	14.00	27.13	3.40	0.85	24.75	5.35	15.39
	0.2% (0.02%)	95.51	0.75	1.05	0.85	8.70	7.00	0.60	2.05	0.75	5.30	2.20	2.97
	Average	95.49	33.51	47.14	43.40	34.50	34.31	46.22	25.31	24.87	44.49	27.42	36.21
All2Random	10% (1%)	95.30	88.74	51.61	99.73	99.73	99.45	41.76	90.05	96.39	99.71	96.80	86.40
	1% (0.1%)	95.52	66.49	52.81	83.70	88.48	89.08	38.89	38.19	53.37	97.09	48.61	65.67
	0.5% (0.05%)	95.50	22.67	18.26	57.18	70.83	77.63	41.38	13.42	10.06	88.59	11.54	41.16
	0.2% (0.02%)	96.15	12.36	32.26	12.36	48.40	54.60	13.48	1.40	0.56	53.89	3.53	23.28
	Average	95.62	47.57	38.73	63.24	76.86	80.19	33.88	35.77	40.09	84.82	40.12	54.13

fine-tuning defense for ViT models while restricting the rest of the defenses to CNNs. More details can be found in the appendix.

4.2. Evaluating and Understanding MTBAs

We first evaluate MTBAs with parallel, sequential, and hybrid-trigger poisonings, respectively. With these experiments, we further reveal the coexisting, overwriting, and cross-activating effects between different triggers.

4.2.1. PARALLEL MTBAs

Recall that, in parallel MTBAs, we inject the 10 triggers all together into the target CIFAR-10 and ImageNet-20 datasets, with each trigger poisoning a unique subset of clean samples. Here, we report the CIFAR-10 results while deferring the ImageNet-20 results to the appendix. Table 1 summarizes the attack success rate of the 10 triggers under various poisoning rates $\alpha \in [0.2\%, 10\%]$.

Coexisting Effect We first look at the average ASR (last column) result at poisoning rate 10%. One key observation is that these triggers can coexist well in a single model, achieving 98.50%, 88.04%, and 86.40% ASR for All2One, All2All, and All2Random targets, respectively. Most of the triggers demonstrate an ASR of well above 80%, except for the BadNets and Adv triggers under the All2Random attacks. This indicates that fixed trigger patterns (Adv is an adversarially perturbed version of the BadNets checkerboard trigger) may be easily influenced by other triggers. Overall, All2One attacks exhibit a more robust attack performance than All2All or All2Random attacks at this poisoning rate, which is somewhat expected as All2One attacks have the same target.

Moving on to low poisoning rates (0.2% to 1%), we find that the average ASR over all 10 triggers (the last column)

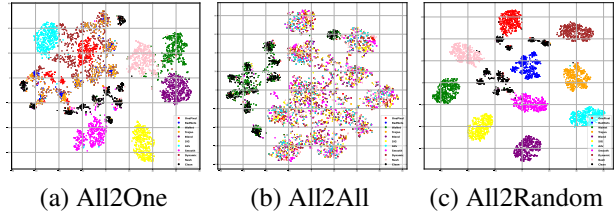


Figure 4. The t-SNE visualizations of parallel MTBAs on ResNet-18 models trained on CIFAR-10. Each color represents the deep representations learned for one type of poisoned samples.

degrades significantly with the poisoning rate. However, there are still survivors at an extremely low poisoning rate of 0.2%, for example, the Blend, SIG, and Dynamic triggers have an ASR $> 40\%$ under the All2One and All2Random settings. No triggers are successful under the All2All setting at this low poisoning rate. We conjecture this is because the cyclic relabeling strategy of All2All causes both local (intra-trigger) and global (inter-trigger) overlaps and disruptions to the ‘trigger-target’ mapping, making it difficult to associate a small fixed trigger to rotated target labels. This result indicates that the All2All setting turns out to be the most challenging attack setting under extremely low poisoning rates (e.g., 0.2% and 0.5%).

The results in Table 1 can also help answer the question as to whether there exists a single strongest trigger in all scenarios. It shows that, under the All2One setting, Dynamic is the strongest trigger on average across different poisoning rates; under the All2All setting, the BadNets trigger is the strongest; while under the All2Random setting, the Dynamic trigger becomes the strongest again. Overall, the Dynamic trigger is the strongest under the All2One and All2Random settings and is close to the best trigger (BadNets) under the All2All setting. Therefore, we believe it has

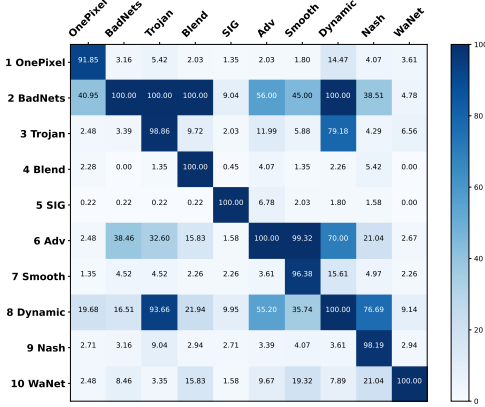


Figure 5. The ASR (%) confusion matrix of sequential multi-trigger attacks on CIFAR-10 (ResNet-18). *Row*: training triggers used to poison the model following the 1 – 9 order; *Column*: testing triggers used to activate the attack at test time.

the potential to be the single strongest trigger. Our experiments with sequential MTBAs in Section 4.2.2 also confirm the hybrid characteristic of the Dynamic trigger, i.e., it can cross-activate other triggers. It is worth mentioning that not all sample-wise triggers are strong, e.g., sample-wise triggers Smooth and WaNet are weaker than dataset-wise trigger BadNets under the All2One and All2All settings.

To help understand the clusters formed by different triggers, we show the t-SNE (Van der Maaten & Hinton, 2008) plots of the 10 triggers under the All2One, All2All, and All2Random label modifications in Figure 4. It shows distinctive clustering effects under the three label modification strategies. Specifically, there exist both small compact clusters and relatively large clusters for All2One and All2Random attacks, yet no meaningful clusters for All2All attacks. This confirms that All2All attacks are indeed harder to achieve, highlighting the most complex attacking scenario. The independent clusters learned by the model for different triggers explain the coexisting effect between different triggers.

4.2.2. SEQUENTIAL MTBAS

Overwriting Effect Sequential MTBAs involve the injection of the 10 triggers following a specified order for iterative training epochs (every 10 epochs). The injection order and the attack performance after each trigger was implanted into the model are illustrated in the form of a confusion matrix in Figure 5. As can be observed, there exists an *overwriting effect* in sequential MTBAs, i.e., the effective trigger before became ineffective after new triggers were injected into the model. For instance, OnePixel drops from 91.85% ASR to 40.95% after BadNets was injected into the model, and further drops to 2.48% after Trojan was injected. The same effect is also observed for almost all triggers, indicated



Figure 6. Example hybrid triggers composed of 4 trigger patterns (BadNets, Dynamic, Nash, and WaNet) on CIFAR-10 images.

by the consistent trend where the cells below the diagonal cells all have lower ASRs.

Cross-activating Effect Another important observation is that certain rows have consistently higher ASRs (more blue cells), for example, the BadNets, Adv, and Dynamic rows. This is a *cross-activating phenomenon*, that is, one type of trigger was frequently activated by other types of triggers. This supervising effect implies that the triggers share certain or even high similarities. For example, BadNets (the 2nd row in Figure 5) can be activated by BadNets, Trojan, Blend, Adv, Smooth, Dynamic, and Nash, with an ASR of 100%, 100%, 100%, 56%, 45%, 100%, and 38.51%, respectively. The Dynamic trigger can be activated by Trojan, Adv, Smooth, Dynamic, and Nash with an ASR of 93.66%, 55.20%, 35.74%, 100%, and 76.69%, respectively. We speculate that the cross-activating effect is a result of similar pixel distributions in the trigger patterns, like those shared among BadNets, Trojan, and Dynamic triggers. Amongst the triggers, Trojan and Dynamic are the two most similar triggers, i.e., Trojan can activate Dynamic by an ASR of 93.66% while Dynamic can activate Trojan by 79.18%. This is because both triggers are optimized triggers. We believe these subtle but intriguing relationships between different triggers deserve more in-depth investigation, especially under the multi-trigger setting.

4.3. Hybrid-trigger MTBAs

Different from parallel and sequential MTBAs where the triggers are independent, our hybrid-trigger attack mixes multiple triggers into a single clean sample, all pointing to the same backdoor target label. Figure 6 shows example of the hybrid triggers. This section explores the effectiveness of our hybrid-trigger attack on the CIFAR-10 dataset. To ensure high attack performance, we chose four triggers to construct the hybrid trigger, including one static trigger BadNets, one Dynamic, and two invisible triggers Nash and WaNet. Note that the Dynamic trigger does not work well as part of a hybrid. We apply those triggers in a random order (we will show that the order has minimum impact on

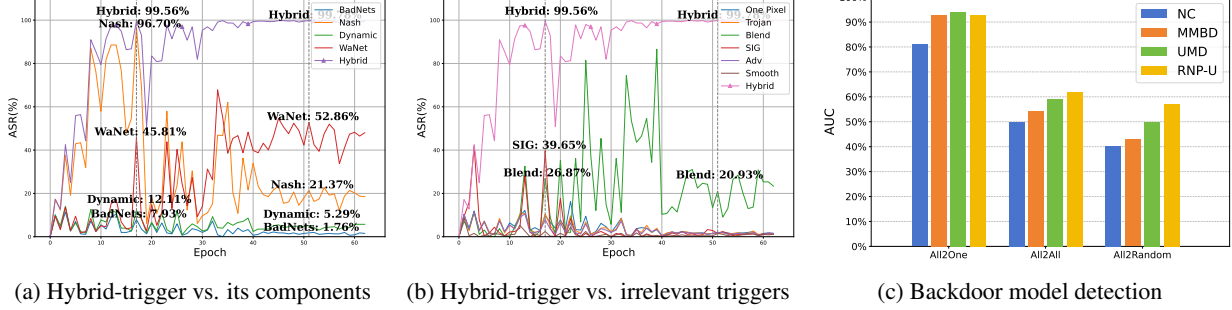


Figure 7. The ASR (%) of hybrid-trigger attack vs. its component triggers (a) and vs. other unrelated triggers (b), at different training epochs of the target model. (c) The backdoor model detection performance (AUROC) of different detection methods.

Table 2. The performance (remaining ASR, %) of 4 backdoor removal methods against the parallel multi-trigger attacks with total 10% (trigger-wise 1%) poisoning rate under the All2One, All2All, and All2Random modes. The experiments were done on CIFAR-10 using only 1% (500) clean samples as the defense data.

Backdoor Removal	No Defense			FT			FP			NAD			ANP		
	All2One	All2All	All2Random												
Clean Acc.	93.98	93.44	93.2	91.40	91.80	91.10	83.00	87.60	86.80	85.50	85.40	87.18	85.30	86.60	86.40
OnePixel	94.83	77.80	91.95	88.51	77.00	91.95	49.01	67.10	65.11	30.10	42.10	63.11	0.00	73.10	88.51
BadNets	100.00	81.00	55.68	28.12	75.33	54.55	22.91	52.38	39.42	12.91	20.38	34.32	1.10	74.18	65.53
Trojan	100.00	82.60	100.00	92.9	78.78	95.51	50.11	72.10	92.78	11.31	59.12	62.78	2.20	77.11	95.51
Blend	99.56	77.20	100.00	99.12	25.13	100.00	78.81	74.30	96.13	32.09	38.32	56.13	11.00	22.33	72.53
SIG	99.34	88.00	100.00	98.9	51.31	100.00	87.80	83.31	97.51	47.60	32.31	37.51	42.86	43.12	90.12
Adv	100.00	81.00	39.41	19.22	75.52	31.82	43.40	42.22	43.52	23.20	68.32	43.52	13.10	74.62	83.55
Smooth	93.40	81.20	94.62	83.52	72.78	95.70	69.23	57.80	86.28	22.75	65.80	86.28	1.10	91.00	98.92
Nash	100.00	88.40	96.74	83.8	75.50	94.57	85.71	51.20	91.54	33.71	84.22	91.54	13.19	89.51	93.48
Dynamic	97.37	89.66	100.00	97.6	81.11	100.00	97.10	78.93	99.11	68.41	67.38	99.11	7.69	65.53	100.00
WaNet	97.59	77.60	100.00	95.3	69.13	98.72	66.79	63.21	89.33	25.78	57.48	54.53	5.14	64.92	3.04
Average	98.21	82.45	88.33	79.85	70.31	86.28	65.09	64.26	80.07	30.79	53.54	62.88	9.74	67.54	79.12

the ASR) using a soft blending approach. The examples of hybrid-trigger are shown in appendix.

Figure 7a illustrates the ASR of our hybrid-trigger attack and individual triggers. One key observation is that the hybrid trigger can not only achieve a high ASR ($\geq 90\%$) but also demonstrate a strong cross-activating effect on its component triggers (not all of them though). Particularly, besides the hybrid trigger, the ASR of Nash and WaNet reaches rapidly 96.70% and 45.81% respectively in the early stage of training (before 20 epochs), although they stabilize at 52.86% and 21.37% respectively in the end. Figure 7b shows a rather surprising phenomenon that the hybrid trigger can even cross-activate the Blend and SIG triggers in the middle of the training, even though they are not part of the hybrid trigger. Unfortunately, this cross-activation is temporary and disappears at the end of the training. We believe designing more advanced hybrid triggers that can cross-activate many other individual triggers is an interesting future direction.

4.4. Re-evaluating Existing Defenses

This section examines the reliability of existing backdoor defense methods against multi-trigger attacks. Here, we re-evaluate 4 backdoor model detection methods and 4 backdoor removal methods. We only focus on parallel poisoning, i.e., the 10 triggers considered in this work were injected in

parallel into the dataset.

Backdoor Model Detection Figure 7c presents the detection AUROC of 4 advanced backdoor model detection methods, including NC, MMBD, UMD, and RNP-U. As can be observed, the four detection methods perform well on All2One multi-trigger attacks, yet perform poorly on All2All and All2Random attacks. Specifically, the detection AUROC deteriorates by nearly 50% and 40% on All2All and All2Random attacks respectively, when compared to that on All2One attacks. Such a huge degradation challenges the reliability of the four detection models under more complex scenarios with unfixed adversarial targets. Out of the four methods, RNP-U consistently outperforms the other three methods, which validates the usefulness of unlearning the benign features before detecting the backdoor features. Meanwhile, although these detection methods can detect the backdoor models to some extent, they all fail to identify the backdoor labels of All2All and All2Random attacks.

Backdoor Removal Table 2 reports the defense performance of four backdoor removal methods, including FT, FP, NAD, and ANP. We measure the defense performance by the remaining ASR, the lower the better. None of the defense methods can fully remove the multi-trigger from the model. The average ASRs are still well above 50%, except for NAD and ANP against All2One attacks. Compared to NAD and ANP, fine-tuning and fine-pruning methods FT and FP are

essentially ineffective against multi-trigger attacks, with an ASR > 60%. This is because the presence of multiple triggers prevents effective forgetting of the backdoor correlation during standard fine-tuning. Additionally, the coexistence of multiple triggers leads to inconsistent parameter activations, rendering the activation-based pruning method FP ineffective. The current state-of-the-art defense method ANP performs poorly on All2All and All2Random attacks, limiting its practicability against more realistic attacks that have different target labels. Clean accuracy (CA) is another perspective looking into the effectiveness of the defense method. The four backdoor removal methods cause a significant reduction in the model’s clean accuracy when facing multi-trigger attacks. Specifically, against All2One attacks, FP, NAD, and ANP reduce the model’s CA by 10.98%, 8.48%, and 8.68% respectively, significantly impairing the functionality of the model. Based on these results, we conclude that existing backdoor detection and removal methods struggle to address the threat of multi-trigger attacks, and developing more advanced countermeasures is imperative. More results of the removal performance for ViT models are deferred into appendix.

5. Conclusion

This work promotes the concept of multi-trigger backdoor attacks (MTBAs) where multiple adversaries may use different types of triggers to poison the same dataset. By designing three poisoning strategies, including parallel, sequential, and hybrid-trigger poisonings, we conducted extensive experiments to study the properties of multi-trigger attacks with 10 representative triggers. Through these experiments, we revealed the coexisting, overwriting, and cross-activating effects of multi-trigger attacks. We also showed the limitations of existing defense methods in detecting and removing multiple triggers from a backdoored model. We hope our work can help reshape future backdoor research towards more realistic settings.

References

Barni, M., Kallas, K., and Tondi, B. A new backdoor attack in cnns by training set corruption without label poisoning. In *ICIP*, 2019.

Chan, W., Jaitly, N., Le, Q., and Vinyals, O. Listen, attend and spell: A neural network for large vocabulary conversational speech recognition. In *ICASSP*, 2016.

Chen, B., Carvalho, W., Baracaldo, N., Ludwig, H., Edwards, B., Lee, T., Molloy, I., and Srivastava, B. Detecting backdoor attacks on deep neural networks by activation clustering. In *AAAI Workshop*, 2019.

Chen, X., Liu, C., Li, B., Lu, K., and Song, D. Targeted backdoor attacks on deep learning systems using data poisoning. *arXiv preprint arXiv:1712.05526*, 2017.

Cheng, S., Liu, Y., Ma, S., and Zhang, X. Deep feature space trojan attack of neural networks by controlled detoxification. In *AAAI*, 2021.

Deng, J., Dong, W., Socher, R., Li, L.-J., Li, K., and Fei-Fei, L. Imagenet: A large-scale hierarchical image database. In *CVPR*, 2009.

Devlin, J., Chang, M.-W., Lee, K., and Toutanova, K. Bert: Pre-training of deep bidirectional transformers for language understanding. In *NAACL*, 2019.

Dosovitskiy, A., Beyer, L., Kolesnikov, A., Weissenborn, D., Zhai, X., Unterthiner, T., Dehghani, M., Minderer, M., Heigold, G., Gelly, S., et al. An image is worth 16x16 words: Transformers for image recognition at scale. 2021.

Gao, Y., Xu, C., Wang, D., Chen, S., Ranasinghe, D. C., and Nepal, S. Strip: A defence against trojan attacks on deep neural networks. In *ACSAC*, 2019.

Gu, T., Dolan-Gavitt, B., and Garg, S. Badnets: Identifying vulnerabilities in the machine learning model supply chain. *arXiv preprint arXiv:1708.06733*, 2017.

Guo, W., Wang, L., Xing, X., Du, M., and Song, D. Tabor: A highly accurate approach to inspecting and restoring trojan backdoors in ai systems. *arXiv preprint arXiv:1908.01763*, 2019.

He, K., Zhang, X., Ren, S., and Sun, J. Deep residual learning for image recognition. In *CVPR*, 2016.

Howard, A. G., Zhu, M., Chen, B., Kalenichenko, D., Wang, W., Weyand, T., Andreetto, M., and Adam, H. Mobilenets: Efficient convolutional neural networks for mobile vision applications. *arXiv preprint arXiv:1704.04861*, 2017.

Huang, H., Ma, X., Erfani, S., and Bailey, J. Distilling cognitive backdoor patterns within an image. *ICLR*, 2023.

Huang, K., Li, Y., Wu, B., Qin, Z., and Ren, K. Backdoor defense via decoupling the training process. In *ICLR*, 2022.

Li, Y., Zhai, T., Wu, B., Jiang, Y., Li, Z., and Xia, S. Rethinking the trigger of backdoor attack. *arXiv preprint arXiv:2004.04692*, 2020.

Li, Y., Li, Y., Wu, B., Li, L., He, R., and Lyu, S. Invisible backdoor attack with sample-specific triggers. In *ICCV*, pp. 16463–16472, 2021a.

Li, Y., Lyu, X., Koren, N., Lyu, L., Li, B., and Ma, X. Anti-backdoor learning: Training clean models on poisoned data. In *NeurIPS*, 2021b.

Li, Y., Lyu, X., Koren, N., Lyu, L., Li, B., and Ma, X. Neural attention distillation: Erasing backdoor triggers from deep neural networks. In *ICLR*, 2021c.

Li, Y., Jiang, Y., Li, Z., and Xia, S.-T. Backdoor learning: A survey. *TNNLS*, 2022.

Li, Y., Lyu, X., Ma, X., Koren, N., Lyu, L., Li, B., and Jiang, Y.-G. Reconstructive neuron pruning for backdoor defense. In *ICML*, 2023.

Lin, J., Xu, L., Liu, Y., and Zhang, X. Composite backdoor attack for deep neural network by mixing existing benign features. In *CCS*, 2020.

Liu, K., Dolan-Gavitt, B., and Garg, S. Fine-pruning: Defending against backdooring attacks on deep neural networks. In *RAID*, 2018a.

Liu, Y., Ma, S., Aafer, Y., Lee, W.-C., Zhai, J., Wang, W., and Zhang, X. Trojaning attack on neural networks. In *NDSS*, 2018b.

Liu, Y., Lee, W.-C., Tao, G., Ma, S., Aafer, Y., and Zhang, X. Abs: Scanning neural networks for back-doors by artificial brain stimulation. In *Proceedings of the 2019 ACM SIGSAC Conference on Computer and Communications Security*, pp. 1265–1282, 2019.

Liu, Y., Ma, X., Bailey, J., and Lu, F. Reflection backdoor: A natural backdoor attack on deep neural networks. In *ECCV*, 2020.

Mann, B., Ryder, N., Subbiah, M., Kaplan, J., Dhariwal, P., Neelakantan, A., Shyam, P., Sastry, G., Askell, A., Agarwal, S., et al. Language models are few-shot learners. 2020.

Nguyen, A. and Tran, A. Input-aware dynamic backdoor attack. In *NeurIPS*, 2020.

Nguyen, A. and Tran, A. Wanet-imperceptible warping-based backdoor attack. In *ICLR*, 2021.

Tran, B., Li, J., and Madry, A. Spectral signatures in backdoor attacks. In *NeurIPS*, 2018.

Turner, A., Tsipras, D., and Madry, A. Clean-label backdoor attacks. <https://people.csail.mit.edu/madry/lab/>, 2019.

Van der Maaten, L. and Hinton, G. Visualizing data using t-sne. *Journal of machine learning research*, 9(11), 2008.

Wang, B., Yao, Y., Shan, S., Li, H., Viswanath, B., Zheng, H., and Zhao, B. Y. Neural cleanse: Identifying and mitigating backdoor attacks in neural networks. In *S&P*. IEEE, 2019.

Wang, H., Xiang, Z., Miller, D. J., and Kesidis, G. Mm-bd: Post-training detection of backdoor attacks with arbitrary backdoor pattern types using a maximum margin statistic. In *Symposium on Security and Privacy (SP)*, 2023.

Wu, D. and Wang, Y. Adversarial neuron pruning purifies backdoored deep models. *NeurIPS*, 2021.

Xiang, Z., Xiong, Z., and Li, B. Umd: Unsupervised model detection for x2x backdoor attacks. In *ICML*, 2023.

Xu, X., Wang, Q., Li, H., Borisov, N., Gunter, C. A., and Li, B. Detecting ai trojans using meta neural analysis. In *S&P*, 2021.

Xue, M., He, C., Wang, J., and Liu, W. One-to-n & n-to-one: Two advanced backdoor attacks against deep learning models. *TDSC*, 2020.

Zeng, Y., Park, W., Mao, Z. M., and Jia, R. Rethinking the backdoor attacks' triggers: A frequency perspective. In *ICCV*, 2021.

Zheng, R., Tang, R., Li, J., and Liu, L. Data-free backdoor removal based on channel lipschitzness. In *ECCV*, 2022.

A. Experimental Details

All experiments were run on NVIDIA Tesla A100 GPUs with PyTorch implementations. We trained the backdoored models of the CNN architecture from scratch for 60 epochs, using SGD optimizer, batch size 128, weight decay 5×10^{-4} , and an initial learning rate of 0.1 which was decayed to 0.01 at the 40th epoch. For the Transformer architecture, we finetuned the model with publicly available pre-trained weights¹ for 5 to 10 epochs, while injecting the backdoor with a finetuning (learning) rate of 0.001 (other parameters were kept unchanged).

A.1. Datasets and Models

The datasets and DNN models used in our experiments are summarized in Table 3.

Table 3. Datasets and models used in our experiments.

Dataset	Model	No. Classes	Input Size	No. Training Images
CIFAR10	ResNet-18	10	$32 \times 32 \times 3$	50000
	MobileNet-V2	10	$32 \times 32 \times 3$	50000
	ViT-Small	10	$224 \times 224 \times 3$	50000
	ViT-Base	10	$224 \times 224 \times 3$	50000
ImageNet-20 Subset	ResNet-50	20	$224 \times 224 \times 3$	26000
	ViT-Base	20	$224 \times 224 \times 3$	26000

A.2. Attack Configurations

On the CIFAR-10 dataset, we considered 10 prevalent poisoning-based backdoor attack methods, including static triggers like OnePixel (Tran et al., 2018), BadNets (Gu et al., 2017), Trojan attack (Liu et al., 2018b), global triggers like Blend (Chen et al., 2017), Sinusoidal Spectrum (SIG) (Barni et al., 2019), Adversarial Noise (Adv) (Turner et al., 2019), Smooth (Zeng et al., 2021), Nashivell filter (Nash) (Liu et al., 2019), and sample-wise triggers like Dynamic (Nguyen & Tran, 2020), WaNet (Nguyen & Tran, 2021). Figure 8 illustrates 10 types of backdoor triggers and the basic configurations used by these attacks are reported in Table 4. To ensure fair and consistent comparison with previous works, we employed the dirty-label poisoning setting, which involves adding backdoor triggers and modifying the ground truth labels. Due to a fail of reproduction, on the ImageNet dataset, we only considered 5 attacks: BadNets (Gu et al., 2017), Trojan (Liu et al., 2018b), Blend (Chen et al., 2017), and Sinusoidal Spectrum (SIG) (Barni et al., 2019), and Nash (Liu et al., 2019). All backdoored models were trained with standard data augmentation techniques including random crop and horizontal flipping.

To ensure the independent effectiveness of the 10 trigger patterns, we validated the attack success rate (ASR) and accuracy (CA) of each trigger on the CIFAR-10 dataset. The experimental results are shown in Table 5, demonstrating

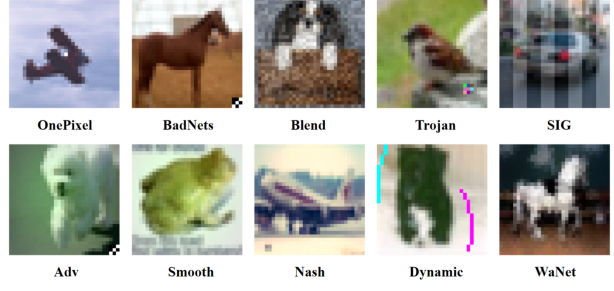


Figure 8. The 10 types of backdoor triggers on CIFAR-10.

that under the single-trigger setting, all attacks reached full (100%) ASR.

Table 4. Configurations of the 10 basic backdoor attacks.

Attacks	Trigger Type	Trigger Size	Trigger Pattern
OnePixel	Static	Pixel	Pixel modification
BadNets	Static	Patch	checkerboard
Trojan	Static	Patch	Reversed watermark
Blend	Global	Full image	Gaussian noise
SIG	Global	Full image	Sinusoidal signal
Adv	Sample-wise	Full image	Noise + checkerboard
Smooth	Global	Full image	Style transfer
Nash	Global	Full image	Instagram filter
Dynamic	Sample-wise	Full image	Mask generator
WaNet	Sample-wise	Full image	Deformation

A.3. Defense Configurations

We considered 8 advanced backdoor defense methods, including 4 backdoored model detection techniques: Neural Cleanse (NC) (Wang et al., 2019), UMD (Xiang et al., 2023), MMBD (Wang et al., 2023), and Unlearning (Li et al., 2023), as well as 4 mainstream backdoor removal techniques, including Fine-tuning (FT), Finepruning (FP) (Liu et al., 2018a), Neural Attention Distillation (NAD) (Li et al., 2021c), and Adversarial Neural Pruning (ANP) (Wu & Wang, 2021). In the case of All defenses had limited access to only 500 clean defense samples.

For the 4 backdoored model detection methods, we used their open-source code and recommended settings. For NC (Wang et al., 2019), we set the learning rate to 0.005 for reverse-engineering the trigger. For MMBD (Wang et al., 2023), we estimated the maximum margin statistic for each category, calculated the p -value, and set the threshold to 0.05 to determine the backdoor model. For UMD (Xiang et al., 2023), we set the learning rate to $1e^{-5}$ to optimize the perturbed images and set $\beta = 0.05$ to compute the threshold. For RNP-U (Li et al., 2023), we unlearned the model with a learning rate of 0.005 and judged the backdoor model with prediction labels.

For the 4 backdoor removal methods, we used their open-

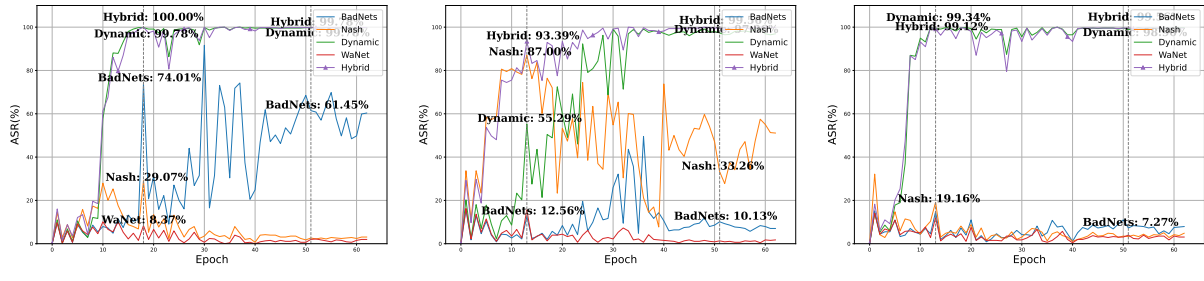
¹<https://github.com/huggingface/pytorch-image-models>

Table 5. The ASR (%) of single-trigger attacks on ResNet-18 and CIFAR-10 dataset. The best results are **boldfaced**.

Single-trigger Attacks	Poisoning Rate							
	CA				ASR			
	Attack	1% (500)	0.1% (50)	0.05% (25)	0.02% (10)	1% (500)	0.1% (50)	0.05% (25)
OnePixel	92.69	92.09	94.79	91.69	94.62	44.23	5.37	1.75
BadNets	93.7	92.79	93	91.6	100	100	11.3	1.1
Trojan	92.99	94.41	91.99	92.99	98.13	16.35	1.53	1.31
Blend	93.7	91.6	94.49	90.99	100	99.88	96.33	84.97
SIG	93	93.29	93.39	91.4	100	96.71	91.09	62.81
Adv	94.19	93.99	91.89	93.49	100	99.1	30.28	0.99
Smooth	91.69	92.6	92.99	92.99	94.9	34.15	16.37	5.84
Nash	93.69	93.39	93.79	91.69	96.18	37.1	12.22	4.15
Dynamic	92.99	94.59	95.19	92.19	99.88	95.94	94.19	19.46
WaNet	93.51	92.89	93.67	93.06	99.23	97.77	59.61	6.98
Average	93.22	93.16	93.52	92.21	98.29	72.12	41.83	18.94

 Table 6. The ASR (%) of parallel multi-trigger attacks on the ImageNet-20 subset. The best results are **boldfaced**.

Label Modification	Model	Parallel Attacks (Poisoning rate 10%)						Parallel Attacks (Poisoning rate 1%)					
		Clean	BadNets	Trojan	Blend	SIG	Nash	Clean	BadNets	Trojan	Blend	SIG	Nash
All2One	ResNet-50	76.90	90.20	18.60	92.40	73.10	92.10	78.50	6.20	6.70	38.20	50.90	52.00
	ViT-Base	93.10	97.90	43.90	99.70	96.90	95.80	93.70	9.30	5.90	91.70	55.20	72.20
	Average	85.00	94.05	31.25	96.05	85.00	93.95	86.10	7.75	6.30	64.95	53.05	62.10
All2All	ResNet-50	75.50	47.80	16.10	52.20	39.80	54.10	80.00	3.90	4.70	11.10	10.40	12.60
	ViT-Base	93.70	91.60	38.50	89.70	86.10	86.90	94.10	24.50	2.50	41.30	22.40	34.90
	Average	84.60	69.70	27.30	70.95	62.95	70.50	87.05	14.20	3.60	26.20	16.40	23.75
All2Random	ResNet-50	76.60	83.90	20.10	95.50	69.30	92.00	76.30	6.90	5.80	38.80	39.60	62.20
	ViT-Base	93.60	99.00	46.60	99.80	96.10	97.70	93.80	70.30	5.60	94.00	72.40	64.20
	Average	85.10	91.45	33.35	97.65	82.70	94.85	85.05	38.60	5.70	66.40	56.00	63.20



(a) BadNets, Dynamic, Nash, and WaNet (b) BadNets, Nash, Dynamic, and WaNet (c) Dynamic, WaNet, BadNets, and Nash

Figure 9. Hybrid-trigger attacks with different trigger stacking orders.

source code and carefully adjusted hyperparameters to achieve the best defense performance. For FT, we fine-tuned the model for 10 epochs with a learning rate of 0.05, 0.01, and 0.001. We re-implemented FP (Liu et al., 2018a) using PyTorch and pruned the last convolutional layer (i.e., Layer4.conv2) of the model. For NAD (Li et al., 2021c), we cautiously selected the best hyperparameter β from [0, 5000]. For ANP (Wu & Wang, 2021), we used their open-source code with the recommended settings, with the perturbation budget set to $\epsilon = 0.4$ and the trade-off coefficient to $\alpha = 0.2$. We determined the optimal pruning threshold based on grid search. All the above defense techniques used the same data augmentation techniques as model training, i.e., random crop and horizontal flipping.

B. More Experimental Results

B.1. Parallel MTBAs on the ImageNet Subset

Table 6 displays the performance of parallel MTBAs on the ImageNet-20 subset. The experimental results are consistent with that on CIFAR-10. Particularly, most of the triggers can coexist with each other at a high poisoning rate (10%), together achieving a high ASR above 80%. Notably, with an increase in image scale and resolution, the ASR of full-image triggers (Blend, SIG, and Nash) surpasses that of the local triggers (BadNets and Trojan) at a low poisoning rate (1%). We suspect that the full image triggers are somewhat enhanced on high-resolution images, rendering the backdoor features more prominent and easier to learn.

B.2. Hybrid-trigger MTBAs with Different Trigger Stacking Orders

To further explore the cross-activating effect of hybrid-trigger attacks, here we investigated the impact of three different trigger stacking orders with 4 trigger patterns (BadNets, Dynamic, Nash, and WaNet). As shown in Figure 9(a)-(c), we find that 1) the stacking order of the triggers can impact the cross-activating effect. Specifically, the cross-activating effect of a previous trigger may be overwritten or compromised by a subsequent trigger; and 2) the Dynamic trigger exhibits a generally stronger cross-activating capability than others, maintaining high ASR under different stacking orders. Figure 6 provides a few examples of the hybrid triggers attached to the CIFAR-10 images.

B.3. Defense Results on ViTs

Since most existing defense methods were originally designed for CNNs, here we only test the fine-tuning (FT) defense on ViT models. Table 7 reports the defense results of FT against parallel MTBAs (at a poisoning rate of 10%) on the ViT-base model. It is clear that FT is ineffective in defending against parallel MTBAs on ViT, even with differ-

ent learning rates. The remaining ASRs are still above 80% for 8/12 of the cases. Therefore, how to design effective defense methods for ViT models against parallel MTBAs has become a challenging but imperative task.

B.4. Parallel MTBAs on Different Models

Tables 8, 9, 10, and 11 report the attack performance of parallel MTBAs on the 4 model architectures (2 CNNs and 2 ViTs) at a poisoning rate of 10%, 1%, 0.5% and 0.2%, respectively.

It shows that most triggers can coexist in different model architectures at a high poisoning rate of 10%, but exhibit varied ASRs when the poisoning rate becomes low, e.g., 0.2%.

Table 7. The defense performance (remaining ASR, %) of fine-tuning (FT) against the parallel MTBAs on ViT-base model at poisoning rate 10% (each trigger poisons 1%). The experiments were done on CIFAR-10 using only 1% (500) clean samples as the defense data.

Backdoor Removal	No Defense			FT (lr=0.05)			FT (lr=0.01)			FT (lr=0.001)		
	All2One	All2All	All2Random	All2One	All2All	All2Random	All2One	All2All	All2Random	All2One	All2All	All2Random
Clean Acc.	98.68	98.44	98.50	98.60	90.44	98.00	96.46	98.20	97.50	98.72	98.34	98.20
OnePixel	93.86	84.40	84.71	93.91	82.40	78.65	85.96	60.60	75.29	90.85	76.20	91.95
BadNets	100.00	97.20	52.87	100.00	93.40	59.78	100.00	89.20	50.57	99.77	93.80	52.69
Trojan	100.00	95.20	98.90	100.00	94.60	98.81	100.00	53.40	97.80	99.77	83.80	95.74
Blend	99.34	84.00	100.00	99.55	78.60	97.87	91.23	45.80	93.26	99.08	75.00	98.80
SIG	99.78	89.80	100.00	99.77	87.00	100.00	99.56	35.20	100.00	99.31	68.60	100.00
Adv	100.00	97.20	35.16	100.00	93.40	27.59	100.00	89.20	37.36	99.77	93.80	37.63
Smooth	97.59	86.40	90.11	97.97	85.80	56.38	91.45	28.60	73.63	94.51	62.80	78.02
Nash	98.90	89.80	93.41	98.42	90.00	79.12	1.54	7.00	74.73	94.05	65.20	84.62
Dynamic	100.00	95.00	100.00	100.00	93.40	98.85	100.00	84.60	100.00	100.00	91.00	100.00
WaNet	98.68	84.20	92.05	99.10	84.60	62.64	52.19	14.40	69.32	93.36	58.60	87.50
Average	98.82	90.32	84.72	98.87	88.32	75.97	82.19	50.80	77.20	97.05	76.88	82.70

Table 8. The ASR (%) of parallel MTBAs at the poisoning rate of 10%. The experiment results were averaged on CIFAR-10. The best results are **boldfaced**.

Label Modification	Model	Parallel MTBAs (poisoning rate 10%)										
		Clean Acc.	OnePixel	BadNets	Trojan	Blend	SIG	Adv	Smooth	Nash	Dynamic	WaNet
All2One	ResNet-18	92.88	94.53	100.00	99.34	100.00	99.56	99.00	93.22	96.28	100.00	97.59
	MobileNet-V2	93.08	95.13	100.00	99.78	99.12	99.12	100.00	93.58	98.45	100.00	99.55
	VIT-Small	98.32	94.75	100.00	99.78	99.78	99.78	100.00	98.25	98.69	100.00	97.12
	VIT-Base	98.46	91.76	100.00	100.00	99.55	99.78	100.00	98.66	98.89	100.00	97.77
	Average	95.69	94.04	100.00	99.73	99.61	99.56	99.75	95.93	98.08	100.00	98.01
All2All	ResNet-18	90.66	76.40	86.00	85.40	70.80	76.60	85.00	71.00	75.80	82.20	75.60
	MobileNet-V2	92.96	86.20	92.80	91.40	76.00	83.60	91.80	82.20	84.20	86.80	84.40
	VIT-Small	98.26	86.80	98.20	97.60	90.40	95.20	97.20	90.80	94.00	96.80	90.60
	VIT-Base	98.54	83.60	98.00	98.40	94.00	96.00	97.10	91.20	93.00	96.80	88.00
	Average	95.11	83.25	93.75	93.20	82.80	87.85	92.75	83.80	86.75	90.65	84.65
All2Random	ResNet-18	92.00	89.01	43.01	100.00	100.00	98.90	47.73	88.17	95.56	100.00	96.51
	MobileNet-V2	92.60	89.01	53.76	98.90	100.00	98.90	42.05	88.17	95.56	100.00	98.84
	VIT-Small	98.60	87.91	54.84	100.00	98.90	100.00	39.77	91.40	97.78	100.00	96.51
	VIT-Base	98.00	89.01	54.84	100.00	100.00	100.00	37.50	92.47	96.67	98.84	95.35
	Average	95.30	88.74	51.61	99.73	99.73	99.45	41.76	90.05	96.39	99.71	96.80

Table 9. The ASR (%) of parallel MTBAs at the poisoning rate of 1%. The experiment results were averaged on CIFAR-10. The best results are **boldfaced**.

Label Modification	Model	Parallel MTBAs (poisoning rate 1%)										
		Clean Acc.	OnePixel	BadNets	Trojan	Blend	SIG	Adv	Smooth	Nash	Dynamic	WaNet
All2One	ResNet-18	92.62	70.18	100.00	77.80	99.78	92.38	99.10	46.19	20.63	98.21	76.01
	MobileNet-V2	93.16	80.00	100.00	92.73	98.86	94.55	100.00	38.64	20.91	98.41	71.36
	VIT-Small	98.54	77.22	100.00	96.10	85.90	80.91	98.90	56.83	61.82	99.57	72.02
	VIT-Base	98.46	73.25	100.00	98.68	97.81	99.56	99.00	87.06	81.14	100.00	72.81
	Average	95.70	75.16	100.00	91.33	95.59	91.85	99.25	57.18	46.12	99.05	73.05
All2All	ResNet-18	92.78	38.40	80.80	57.80	37.60	36.60	80.45	14.00	13.20	55.60	28.00
	MobileNet-V2	92.62	50.60	80.60	65.80	36.60	32.80	81.60	13.40	11.80	57.80	27.60
	VIT-Small	98.4	17.60	35.60	44.40	14.00	15.60	33.30	4.80	1.80	47.40	4.20
	VIT-Base	98.66	45.60	65.00	69.40	30.40	28.60	62.20	15.80	17.80	68.20	10.20
	Average	95.62	38.05	65.50	59.35	29.65	28.40	64.39	12.00	11.15	57.25	17.50
All2Random	ResNet-18	92.10	67.01	49.44	60.87	98.88	91.95	44.44	32.97	49.44	96.51	41.11
	MobileNet-V2	92.70	68.04	88.76	82.61	98.88	81.61	6.67	38.46	29.21	93.02	62.22
	VIT-Small	98.40	59.79	59.55	95.65	68.54	100.00	28.89	38.46	62.92	100.00	42.22
	VIT-Base	98.90	71.13	13.48	95.65	87.64	82.76	75.56	42.86	71.91	98.84	48.89
	Average	95.52	66.49	52.81	83.70	88.48	89.08	38.89	38.19	53.37	97.09	48.61

Table 10. The ASR (%) of parallel MTBAs at the poisoning rate of 0.5%. The experiment results were averaged on CIFAR-10. The best results are **boldfaced**.

Label Modification	Model	Parallel MTBAs (poisoning rate 0.5%)										
		Clean Acc.	OnePixel	BadNets	Trojan	Blend	SIG	Adv	Smooth	Nash	Dynamic	WaNet
All2One	ResNet-18	92.88	52.71	100.00	63.80	99.32	90.05	93.10	8.37	19.00	96.15	42.31
	MobileNet-V2	92.14	55.29	100.00	83.15	99.14	76.67	97.20	9.72	8.42	96.98	27.43
	VIT-Small	98.54	63.24	98.17	95.89	67.58	76.71	97.11	14.84	13.70	99.09	14.16
	VIT-Base	98.56	37.25	87.36	86.92	62.31	76.72	83.63	13.97	29.27	99.56	8.87
	Average	95.53	52.12	96.38	82.44	80.04	92.76	92.76	11.72	17.60	97.94	23.19
All2All	ResNet-18	92.82	25.00	62.20	26.00	32.20	25.80	60.12	4.60	1.40	32.80	12.00
	MobileNet-V2	92.66	22.60	43.60	33.80	23.40	15.40	41.30	4.60	1.40	32.00	7.60
	VIT-Small	98.7	0.00	0.20	3.00	3.80	6.60	0.20	1.60	2.10	13.80	0.60
	VIT-Base	98.74	0.40	7.00	18.00	8.00	8.20	6.90	2.80	0.40	20.40	1.20
	Average	95.73	12.00	28.25	20.20	16.85	14.00	27.13	3.40	0.85	24.75	5.35
All2Random	ResNet-18	93.20	34.88	42.70	37.23	83.33	89.47	45.98	7.37	3.45	92.39	2.20
	MobileNet-V2	91.50	55.81	0.00	67.02	92.86	77.89	100.00	9.47	5.75	94.57	27.47
	VIT-Small	98.20	0.00	1.12	47.87	53.57	69.47	0.00	15.79	4.60	78.26	9.89
	VIT-Base	99.10	0.00	29.21	76.60	53.57	73.68	19.54	21.05	26.44	89.13	6.59
	Average	95.50	22.67	18.26	57.18	70.83	77.63	41.38	13.42	10.06	88.59	11.54

Table 11. The ASR (%) of parallel MTBAs at the poisoning rate of 0.2%. The experiment results were averaged on CIFAR-10. The best results are **boldfaced**.

Labeling Mode	Model	Parallel MTBAs (poisoning rate 0.2%)										
		Clean Acc.	OnePixel	BadNets	Trojan	Blend	SIG	Adv	Smooth	Nash	Dynamic	WaNet
All2One	ResNet-18	93.62	27.80	99.33	21.52	80.94	70.40	93.13	3.36	3.36	88.57	8.97
	MobileNet-V2	93.02	2.51	25.74	6.15	90.89	49.20	20.14	1.37	5.24	86.79	10.48
	VIT-Small	98.52	0.23	0.46	53.23	17.28	3.69	0.26	1.61	0.23	88.02	0.69
	VIT-Base	98.60	12.02	45.80	54.65	20.41	76.64	40.10	0.91	0.91	97.73	1.59
	Average	95.94	10.64	42.83	33.89	52.38	49.98	38.40	1.81	2.43	90.28	5.43
All2All	ResNet-18	92.38	1.40	2.20	1.40	19.00	15.20	0.20	4.20	1.00	7.80	3.80
	MobileNet-V2	92.46	1.40	1.80	1.60	11.20	10.60	1.10	3.00	1.60	11.40	4.00
	VIT-Small	98.54	0.20	0.20	0.40	2.80	1.00	1.10	1.00	0.40	0.20	0.80
	VIT-Base	98.64	0.00	0.00	0.00	1.80	1.20	0.00	0.00	0.00	1.80	0.20
	Average	95.51	0.75	1.05	0.85	8.70	7.00	0.60	2.05	0.75	5.30	2.20
All2Random	ResNet-18	93.70	18.39	21.51	14.61	75.53	63.22	53.93	4.49	1.11	83.33	3.26
	MobileNet-V2	93.60	31.03	100.00	11.24	92.55	55.17	0.00	1.12	1.11	37.78	6.52
	VIT-Small	98.40	0.00	0.00	0.00	14.89	22.99	0.00	0.00	0.00	33.33	2.17
	VIT-Base	98.90	0.00	7.53	23.60	10.64	77.01	0.00	0.00	0.00	61.11	2.17
	Average	96.15	12.36	32.26	12.36	48.40	54.60	13.48	1.40	0.56	53.89	3.53